The Island Arc (1998) **7**, 443–459

Thematic Article

Evidence for magma mixing in the Mariana arc system

JAMES K. MEEN,[1] ROBERT J. STERN[2] AND SHERMAN H. BLOOMER[3]

[1]*Department of Chemistry and Texas Center for Superconductivity, University of Houston, Houston, TX 77204–5641,* [2]*Center for Lithospheric Studies, University of Texas at Dallas, Box 830688, Richardson, TX 75083–0688 and* [3]*Department of Geosciences, Oregon State University, Corvallis, OR 97331, USA*

Abstract Volcanoes of the Mariana arc system produce magmas that belong to several liquid lines of descent and that originated from several different primary magmas. Despite differences in parental magmas, phenocryst assemblages are very similar throughout the arc. The different liquid lines of descent are attributed to differences in degree of silica saturation of the primary liquids and in the processes of magmatic evolution (fractional crystallization *vs* magma mixing). Pseudoternary projections of volcanic rocks from several arc volcanoes are used to show differences between different magmatic suites. In most of the arc, parental liquids were Ol- and Hy-normative basalts that crystallized olivine, augite, and plagioclase (± iron-titanium oxide) and then plagioclase and two pyroxenes, apparently at low pressure. Eruptive rocks follow subparallel liquid lines of descent on element–element diagrams and on pseudoternary projections. Magmas at North Hiyoshi are Ne-normative and have a liquid line of descent along the thermal divide due to precipitation of olivine, augite, and plagioclase. Derived liquids are large ion lithophile element (LILE)-rich. Magmas at other Hiyoshi seamounts included an alkaline component but had more complex evolution. Those at Central Hiyoshi formed by a process dominated by mixing alkaline and subalkaline magmas, whereas those at other Hiyoshi seamounts evolved by combined magma mixing and fractional crystallization. Influence of the alkaline component wanes as one goes south from North Hiyoshi. Alkaline and subalkaline magmas were also mixed to produce magmas erupted at the Kasuga seamounts that are behind the arc front. The alkaline magmas at both Hiyoshi and Kasuga seamounts had different sources from those of the subalkaline magmas at those sites as indicated by trace element ratios and by ε_{Nd}.

Key words: liquid lines of descent, magma mixing, petrogenesis, pseudoternary projections.

INTRODUCTION

The present paper investigates the origin of a number of volcanic rocks in the Mariana arc system. While fractional crystallization of tholeiitic and calc-alkaline (subalkaline *in toto*) primary magmas accounts for variation in much of the arc, primary magmas at some arc volcanoes were Ne-normative. In addition, other igneous rocks formed from magmas produced by mixing mafic or intermediate liquids.

Examples of magma mixing from suites of arc-related igneous rocks, particularly in areas of thick felsic crust, are numerous but most involve mixing between mafic and felsic magmas. Few cases of mixing of two mafic magmas of differing degrees of silica-saturation have been reported. Jackson (1993) modeled basaltic andesite at Fukujin seamount in the Mariana arc system as mixed tholeiitic basalt and acid andesite. Edwards *et al.* (1991) argued that the potassic series

Accepted for publication February 1998.

at Muriah in Indonesia formed by the mixing of silica-undersaturated and calc-alkaline magmas.

The suggestion of magma mixing requires coexistence of two liquids on different liquid lines of descent (LLD). The presence of distinct LLD with different enrichments in incompatible elements may have one of several origins. Primary magmas may have differed in incompatible-element contents because of variations in either source composition or degree of partial melting. Isobaric fractional crystallization of such magmas produces similar LLD, and abundances of incompatible elements in derived liquids may be used to infer the contents of those elements in the primary magmas and in magmatic sources (Plank & Langmuir 1988). Fractional crystallization of identical primary magmas at different pressures produces a range of LLD. Even though the actual phases that precipitate are the same in each case, their crystallization in different proportions may alter the LLD profoundly (Meen 1990).

The different LLD that are here suggested for the Mariana arc system apparently formed from discrete primary magmas with different trace element contents. The resultant LLD have very different covariations in elements and the differences are enhanced as evolution progresses.

GEOLOGICAL SETTING AND SAMPLE DESCRIPTIONS

Figure 1 is a map of the Mariana arc system (the Volcano and Mariana arcs) showing locations of the major volcanic provinces. This arc formed in response to subduction of the Pacific plate under the Philippine Sea plate. The Volcano Arc is continuous with the Bonin arc north of 26°N. The extension axis of the Mariana Trough intersects the arc near the location of the Hiyoshi seamounts (Fig. 1) and rifting is apparently propa-

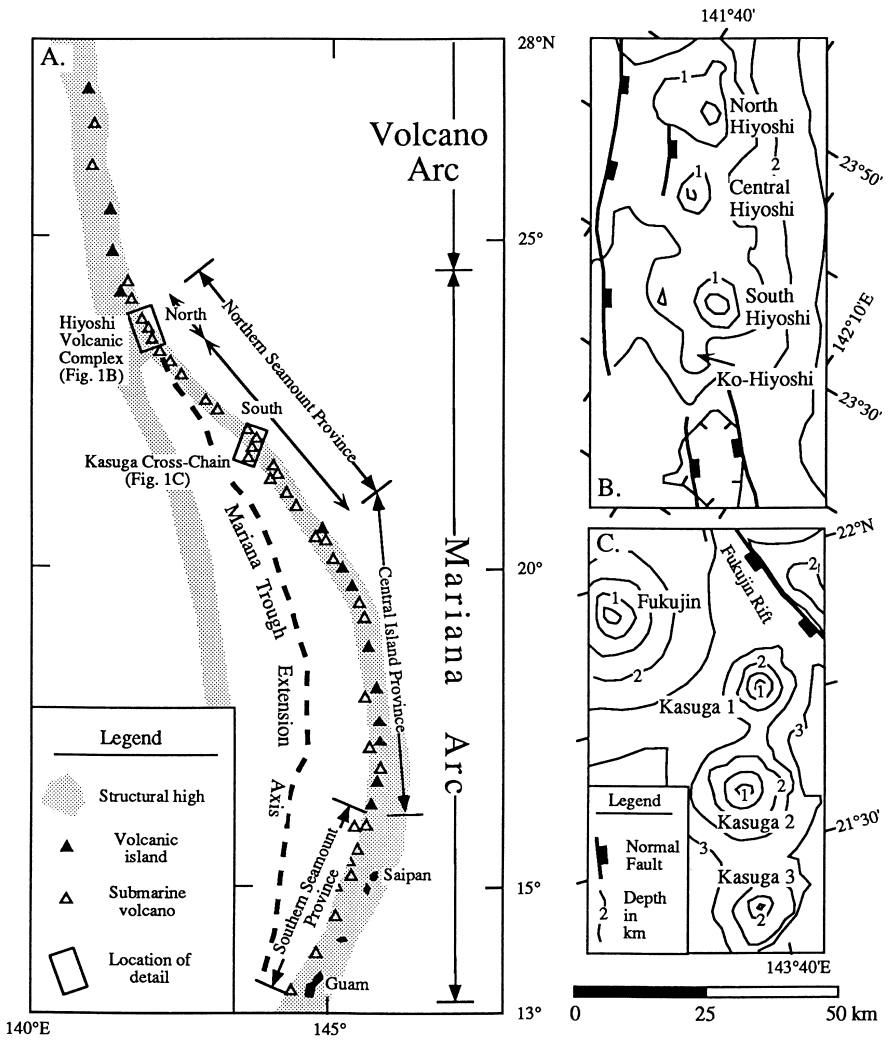

Fig. 1 Location of volcanic provinces in the Mariana arc system (Bloomer *et al.* 1989; Stern *et al.* 1993). (a) Location of major provinces and distribution of volcanoes. Also shown are positions of the detailed maps (b,c). The northern end of the Mariana Trough extension axis intersects the arc just south of Hiyoshi Volcanic Complex. (b) Detail of Hiyoshi Volcanic Complex. (c) Detail of Kasuga Cross-Chain. The scale in lower right applies to Fig. 1(b,c).

gating to the north (Stern *et al.* 1984; Martinez *et al.* 1995).

The Mariana arc consists of three physiographic provinces (Dixon & Stern 1983; Stern *et al.* 1984). Volcanoes in the Northern Seamount Province (NSP, north of 20°30′N) and in the Southern Seamount Province (SSP, south of 16°30′N) are entirely submarine. A few centers in the Central Island Province (CIP, 20°30′N to 16°30′N) are submarine; most are subaerial. Most Mariana arc volcanoes formed on basement of older frontal arc and back-arc basin crust (Hussong & Uyeda 1981; Bloomer *et al.* 1989) that consists of arc tholeiitic basalt, andesite, and dacite of Late Eocene to Miocene age (Reagan & Meijer 1984; Meijer 1980).

The Mariana arc volcanoes have received much attention in the last 20 years (Meijer 1976; Stern 1979, 1981, 1982; Dixon & Batiza 1979; Garcia *et al.* 1979; Chow *et al.* 1980; Meijer & Reagan 1981; Wood *et al.* 1981; Stern & Ito 1983; Dixon & Stern 1983; Stern & Bibee 1984; White & Patchett 1984; Hole *et al.* 1984; Woodhead & Fraser 1985; Ito & Stern 1986; Lin *et al.* 1989, 1990; Woodhead 1989; Jackson 1989; Bloomer *et al.* 1989; Jackson 1993; Stern *et al.* 1993). The most abundant eruptive in the Mariana and Volcano arcs is evolved tholeiitic or calc-alkaline basalt. Andesites are volumetrically minor but rocks as felsic as dacite have been described.

Alkaline lavas with shoshonitic affinities have erupted at Iwo Jima and the Hiyoshi seamounts. Some of these rocks are highly enriched in large ion lithophile elements (LILE) and have biotite phenocrysts (Bloomer *et al.* 1989; Lin *et al.* 1989).

Bloomer *et al.* (1989) described samples from all three provinces of the Mariana arc and from the Volcano arc. They are densely phyric and have glomerophyric and seriate porphyritic textures. Most rocks have phenocryst assemblages of plagioclase, augite, olivine, ± titanomagnetite, ± hypersthene; plagioclase, augite, ± titanomagnetite; plagioclase, augite, hypersthene, ± titanomagnetite. Plagioclase and then augite are the most common phenocrysts. Olivine is most abundant in the CIP and SSP, is rare in volcanic rocks between 20°30′N and 21°25′N, and variable in amount in volcanic rocks further north. Hypersthene occurs in the CIP and south NSP (SNSP), is absent from most of the north NSP (NNSP), and reappears north of Iwo Jima. Some rocks at North Hiyoshi seamount contain biotite phenocrysts.

The Kasuga seamounts form a chain that trends S10°W from the arc front (Fig. 1). The extinct Kasuga 1 (K1) seamount is on the volcanic front south of Fukujin. Kasuga 2 (K2) is 20 km south-southwest of K1 and Kasuga 3 (K3) is another 23 km south. Bloomer *et al.* (1989) described a low-K basaltic andesite from K1. Jackson (1989) studied several rocks from K2 and K3 including very magnesian basalts, dacites, and LILE-enriched absarokites. Stern *et al.* (1993) gave Sr, Nd, Pb, and O isotopic compositions of samples from the Kasuga seamounts.

MAGMA COMPOSITIONAL TRENDS

In the present paper we investigate trends of igneous suites on pseudoternary normative projections because they provide a better means of discriminating between different trends than element–element diagrams. Components are calculated from CIPW norms of whole rocks with iron divided between FeO and Fe_2O_3 by the algorithm of Sack *et al.* (1980), assuming liquids were at 1200 °C at $f(O_2) = NNO$. As well as a projection from Di onto Ol–Pl–Qz/Ne, we project from Di and Pl onto Ol–Or–Qz/Ne. This shows a surface saturated in augite, plagioclase, and one or more of olivine, hypersthene, and quartz.

Figure 2 illustrates an absolute requirement of closed-system fractional crystallization evolution. The parental liquid (PL) in this case is saturated in olivine, plagioclase, and augite and separation of those phases produces a derived liquid (DL). Accumulation of crystals into any liquids in this system results in magma compo-

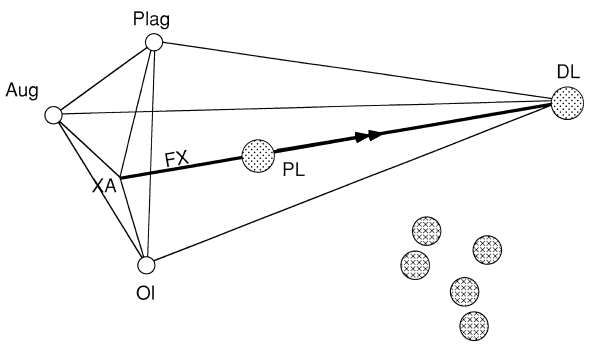

Fig. 2 Schematic representation in an arbitrary phase volume of closed-system fractional crystallization from a parental liquid (PL) to a derived liquid (DL) by removal of olivine (ol), plagioclase (pl), and augite (aug), with a bulk composition XA (crystallizing assemblage). All magma compositions due to closed-system processes must lie in the tetrahedron defined by ol–pl–aug–DL. The cross-hatched circles that lie outside the tetrahedron require an external component.

sitions that lie only in the tetrahedron defined by DL and the compositions of the crystallizing phases. Magmas with compositions outside the tetrahedron require contributions from external sources. All liquids from PL to DL (and beyond) lie on saturation surfaces of olivine, plagioclase, and augite. Additionally, the vector XA–PL–DL shows increase in an incompatible element (or component). The most common representation of such magmatic compositions is in a quaternary with apices Ol, Pl, Di, and an incompatible component (commonly Qz or Ne). In many cases, the quaternary is represented as a projection onto a pseudoternary. One such projection is from Di onto Ol–Pl–Qz/Ne (Fig. 3a).

Liquids saturated in olivine, plagioclase, and augite (L(ol,pl,aug)), and in plagioclase, augite, and low-Ca pyroxene (L(pl,aug,lcp)), are in broad bands in projection from Di onto Ol–Pl–Qz/Ne (Fig. 3a) because of variations in pressure and compositional factors. An increase in pressure causes contraction of the olivine primary phase field so L(ol,pl,aug) moves toward the Ol apex while increases in content of H_2O or K_2O have the opposite effect (Baker & Eggler 1987; Meen 1990). A Hy-normative liquid crystallizing olivine and augite moves away from the Ol (+ Di) apex to attain plagioclase saturation and moves along L(ol,pl,aug) until it begins to crystallize low-Ca pyroxene. Although L(ol,pl,aug,lcp) is at an invariant point in the quaternary system, Ol–Pl–Di–Qz, natural systems have more components and L(ol,pl,aug,lcp) moves to higher Qz as its temperature decreases (Meen 1990). These liquids are in reaction relationship with olivine and when olivine has been consumed (or removed), the liquid can move along L(pl,aug,lcp) to higher Qz.

A LLD along L(ol,pl,aug) does not necessarily indicate that magmas are related by closed-system fractional crystallization. Figure 3(b) shows a mixing trend due to addition of rhyolite to triply saturated basalt on the thermal divide. The trajectory is essentially along L(ol,pl,aug) and L(pl,aug,lcp). In addition, crystallization moves mixed magmas that 'stray' off L(ol,pl,aug) back toward that line. Confinement of magmatic rocks to L(ol,pl,aug) does not prove that members of the suite are related by closed-system processes.

One way of distinguishing between suites produced by fractional crystallization alone and those formed in open systems is by considering the behavior of two incompatible components. We have added Or to the Ol–Pl–Di–Qz/Ne double tetrahedron. Both Or (reflecting K_2O) and either Qz or Ne are incompatible in minerals that precipitate from basaltic liquids. In order to represent compositions in two dimensions, they are projected from both Pl and Di onto Ol–Or–Qz/Ne (Fig. 3c). Fields on this diagram represent saturation in three minerals as labeled, and only liquids that are at least triply saturated can be plotted. A liquid moves directly away from the composition of the crystallizing assemblage. Olivine projects near the Ol apex. Plagioclase consists of albite, anorthite, minor orthoclase and possibly minor excess Al_2O_3 (negative Di) or Qz. Augite dissolves abundant minor components. Jadeite and Ca–Tschermak molecule are recast as Ne and Ab and as An and negative Qz, respectively. Augites also have high contents of enstatite and ferrosilite that are recalculated as Ol and Qz. Augites in alkaline rocks are silica undersaturated or have only minor normative Hy while subalkaline augites have higher Hy : Ol (Fig. 3d). The olivine–plagioclase–augite assemblage that crystallizes from many basaltic and andesitic liquids projects near the Ol apex in this diagram.

Figure 3c cannot represent initial evolution of primary liquids. Only when liquids evolve to crystallize olivine, plagioclase, and augite, can they be shown in this projection. Composition A is a hypothetical multiply saturated liquid that projects to a point similar to those of more mafic subalkaline rocks of the Mariana arc. Separation of olivine, plagioclase, and augite from A produces an LLD directly away from a point near the Ol apex until the liquid reaches L(ol, pl,aug,lcp) at B and then crystallizes plagioclase and two pyroxenes as olivine dissolves. After loss of olivine at C the liquid crystallizes plagioclase and two pyroxenes.

Increase of pressure causes contraction of the olivine primary phase field so L(ol,pl,aug,lcp) moves toward the Ol–Or join. Increase in water content has the opposite effect. The influence of K_2O content on the relative stabilities of olivine and low-Ca pyroxene is shown by the shape of L(ol,pl,aug,lcp).

Curtis (1991) found that a mildly silica-undersaturated (1.6% Ne; 0.8% K_2O) basaltic liquid crystallizes olivine, plagioclase, and augite from 1170 °C to < 1100 °C at 1 atm. During crystallization, the liquid varies little in silica-saturation but becomes greatly enriched in K_2O and other incompatible elements. (Silica-saturation is used

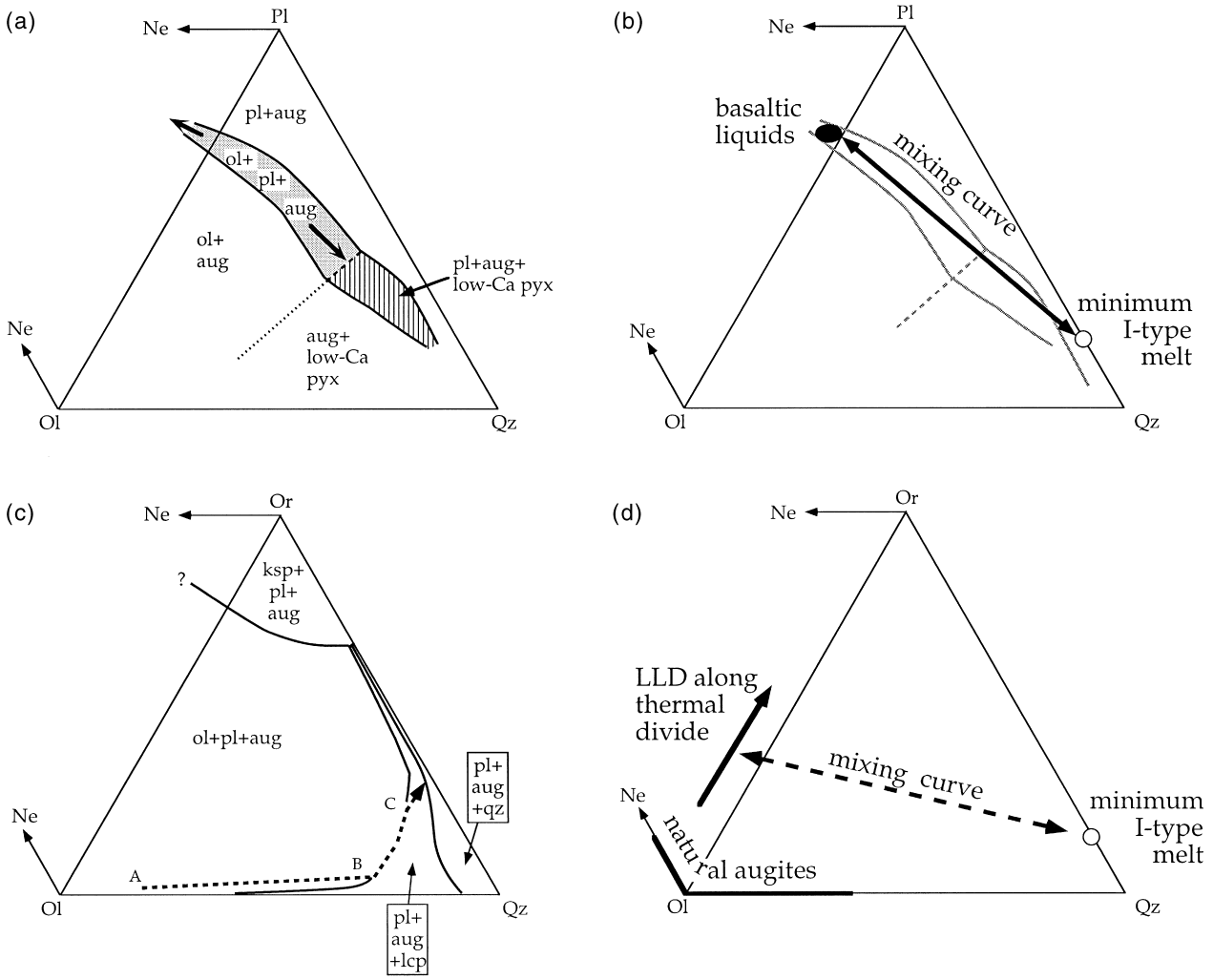

Fig. 3 (a) Compositions of anhydrous liquids saturated in augite and one or more of olivine, plagioclase, and a low-Ca pyroxene at 1 atm projected from diopside (Di) onto the plane nepheline (Ne)–olivine (Ol)–plagioclase (Pl)–quartz (Qz), as interpreted by Meen (1990) for liquids with low-to-moderate potassium contents. Liquids saturated in olivine, plagioclase, and augite, L(ol,pl,aug), lie in the shaded region that is broad due to influences of other chemical parameters on the relative stabilities of olivine and plagioclase. The dashed line denotes the approximate compositions of liquids in equilibrium with olivine, plagioclase, augite, and low-Ca pyroxene (L(ol,pl,aug,lcp)) and the dotted line is L(ol,aug,lcp). The vertically ruled region is L(pl,aug,lcp). The thermal divide due to separation of olivine, plagioclase, and augite is slightly more Qz-rich than the Ol–Pl–Di join but its exact position varies according to other chemical effects. (b) Multiply saturated liquids related by separation of plagioclase, augite and olivine and then low-Ca pyroxene define L(ol,pl,aug) and L(pl,aug,lcp). Magma mixing can also produce these trends. The solid field labeled 'basaltic liquids' shows compositions of some olivine–plagioclase–augite-saturated liquids (Curtis 1991) that lie near the thermal divide. Mixing such liquids with rhyolite (the minimum I-type liquid of White & Chappell 1977) produces a mixing 'curve' that is essentially a straight line along L(ol,pl,aug) and L(pl,aug,lcp). The liquid line of descent (LLD) due to fractional crystallization, due to basalt–rhyolite mixing, and to combined fractional crystallization and assimilation of rhyolite may be similar in this projection. (c) Projections of multiply saturated anhydrous liquids from Di and Pl onto Ne–Ol–orthoclase (Or)–Qz at 1 atm (Meen 1990). The line between ol + pl + aug and the pl + aug + lcp fields defines L(ol,pl,aug,lcp). Point A is the most primitive liquid on a low-K LLD (dashed line) saturated in olivine, plagioclase, and augite. The LLD moves almost directly away from Ol and reaches L(ol,pl,aug,lcp) at B. Liquids stay on that line as long as they are in contact with olivine. The liquid is shown to leave at C but could stay on until saturated in alkali feldspar (ksp). At temperatures below those of C, the liquid crystallizes plagioclase, augite, and low-Ca pyroxene to L(pl,aug,lcp,qz) and can move along that line to the pseudo-eutectic L(pl,aug,lcp,qz,ksp). (d) The line marked 'LLD along thermal divide' was experimentally determined by Curtis (1991) for a mildly alkaline basalt at 1 atm. The LLD, essentially parallel to the critical surface of silica-undersaturation, is due to crystallization along the olivine–augite–plagioclase thermal divide. The dashed line represents mixing curve between a liquid on this line of descent and the rhyolite of Fig. 3(b). Unlike the case in Fig. 3(b), the mixing curve here is not consistent with separation of olivine, plagioclase, and augite.

in the classic sense of Shand (1927). Thus, quartz-bearing or Qz-normative rocks are silica-oversaturated; feldspathoid-bearing or Ne-normative rocks are silica-undersaturated; others are silica-saturated. The join Ol–Pl–Di–Or is the critical surface of silica-undersaturation. Further, 'alkaline' is synonymous with 'Ne-normative' with no reference to total alkali content.) The precipi-

tated augite is slightly more silica-undersaturated than the liquid but olivine and plagioclase are almost exactly silica-saturated, so the crystallized assemblage has a similar degree of silica-undersaturation to that of the liquid. Thus, silica-saturation of the liquids does not change with evolution; liquids apparently remain on the olivine–plagioclase–augite thermal divide. That divide is not a simple ridge but has a broad flat top or even internal 'drainage' so liquid compositions stay on it (Morse 1980).

Addition of felsic melt to mildly alkaline liquids like those produced by Curtis (1991) causes increase in Qz with little change in Or (Fig. 3d). Trends with this orientation cannot be created by separating olivine, plagioclase, and augite only as the trend does not pass through any point that represents a mixture of those three minerals. Such a trend can, however, result from fractional crystallization of a potassic and silica-undersaturated mineral assemblage. One such crystallizing assemblage includes basaltic hornblende, a mineral that typically projects near the critical surface and is mildly potassic. Phase relations of amphibole (± olivine ± plagioclase ± pyroxene) are still imperfectly known but separation of assemblages that include hornblende might well mimic mixing trends in this projection. Amphibole–phyric rocks are not discussed further.

The different orientations of fractional crystallization and magma mixing trends on Fig. 3(c,d) illustrate an advantage of projections in which two components are incompatible in the liquid. Separation of olivine, plagioclase, and augite can produce a wide array of trends (cf. Fig. 3a) depending upon the composition of the parental liquid. All such trends extrapolate to points near the Ol apex. Mixing two liquids creates trends that generally do not pass through the Ol apex and may cross the thermal divide. This allows recognition of many open systems. One exception is mixing between low-K subalkaline magmas (e.g. A on Fig. 3c) and minimum I-type melts that creates trends similar to those due to separation of olivine, plagioclase, and augite. Projections cannot be used to infer the petrogenesis of a single rock; it is the trend of a suite that suggests the process of formation.

We discuss the petrogenesis of some suites in the Mariana system. The relatively simple island-arc tholeiite and calc-alkaline series, discussed first, have compositions consistent with magmas in each suite being related by closed-system fractional crystallization. Alkaline rocks at North Hiyoshi, described next, define a fractional crystallization trend similar to that produced by Curtis (1991). Other volcanic suites near the junction of the Mariana and Volcano arcs apparently formed by mixing magmas that belong to alkaline and subalkaline series. Finally, we will argue that rocks from the Kasuga seamounts also formed by mixing alkaline and subalkaline magmas.

ISLAND-ARC THOLEIITE AND CALC-ALKALINE SERIES IN THE MARIANA ARC SYSTEM

Compositions of igneous rocks from the CIP, Northern Volcano Arc (NVA), and the SNSP projected from Di onto Ol–Pl–Qz are not those of liquids but of liquids and phenocrysts, and some scatter on Fig. 4 is due to their presence. Most rocks contain plagioclase, augite, and olivine, hypersthene or both; in addition, some contain iron–titanium oxide.

The CIP rock that falls nearest the Pl apex contains plagioclase and augite only; the two nearest the Ol apex have >25% olivine + augite phenocrysts that may be cumulative so that the rocks shift toward Ol. The other data lie on a low-pressure LLD due to separation of olivine + augite + plagioclase (L(ol,pl,aug)), then of plagioclase + augite + hypersthene (L(pl,aug,hy)). Four SNSP samples containing only plagioclase and augite project near L(ol,pl,aug,hy). The liquids may have reacted with olivine phenocrysts and they only crystallized minor hypersthene that was not observed.

The projection from Pl and Di onto Ol–Or–Qz (Fig. 5) shows progressive change from saturation in olivine + plagioclase + augite to those phases + hypersthene and to plagioclase + augite + hypersthene. Compositions accord well but not perfectly with low-P experimental phase relations: some rocks in the olivine–plagioclase–augite field contain hypersthene as well as olivine, plagioclase, and augite; others contain hypersthene but no olivine. Fractional crystallization may have occurred at $P > 1$ atm. Alternatively, liquids crystallized to 1 atm L(ol,pl, aug,hy) but accumulated small amounts of plagioclase and pyroxene. Some rocks in the plagioclase–augite–hypersthene field have olivine phenocrysts, which may reflect retention of olivine phenocrysts in liquids no longer saturated in olivine, so olivine and liquid were not in equilibrium. On the other hand, the olivine–plagioclase–

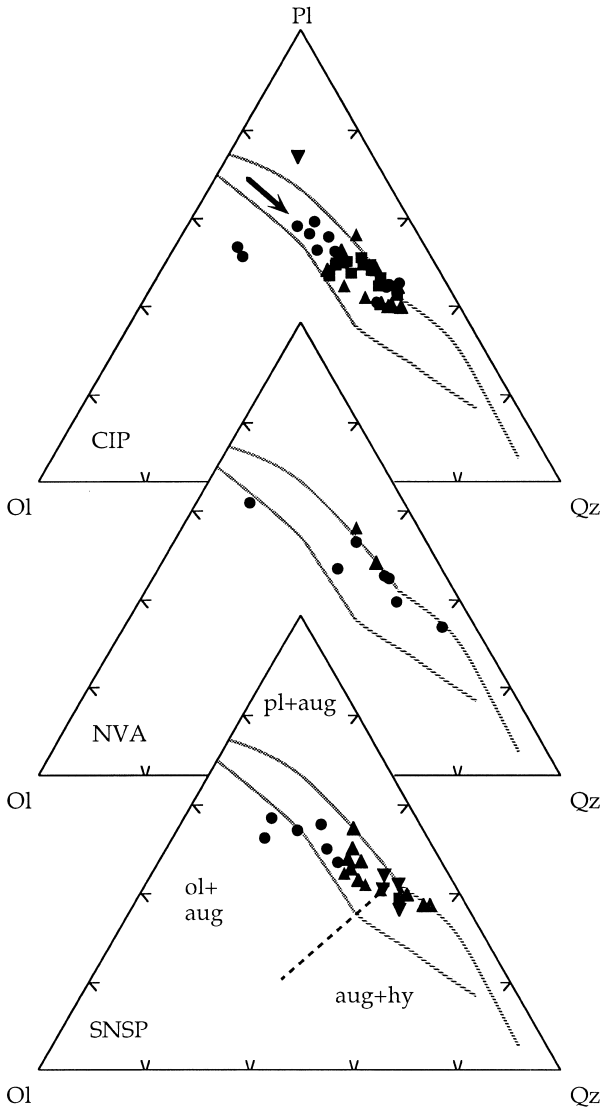

Fig. 4 Compositions of igneous rocks from volcanoes of the Central Island Province (CIP), the Northern Volcano Arc (NVA), and southern part of the Northern Seamount Province (SNSP), from Bloomer *et al.* (1989), projected from Di onto Ol–Pl–Qz. The two lines show positions of L(ol,pl,aug) (gray lines) and L(pl,aug,hy) (dashed lines) at 1 atm. Most data are between the lines, consistent with a liquid line of descent (LLD) along L(ol,pl,aug) from a Hy-normative basaltic liquid with decreasing temperature shown by arrow. (●), ol + pl + aug; (■), ol + pl + aug + hy; (▲), pl + aug + hy; (▼), pl + aug.

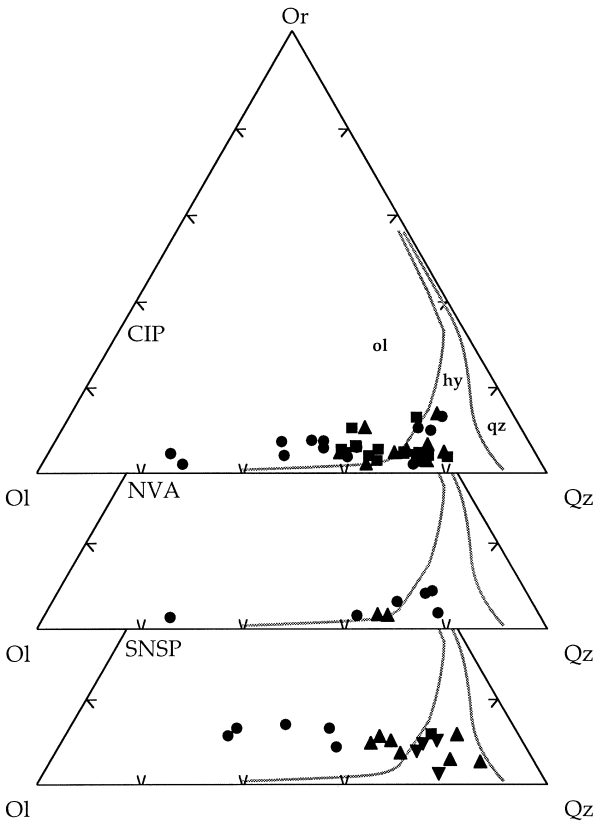

Fig. 5 Igneous rocks of Fig. 4 projected onto Ol–Or–Qz from Pl and Di. The lines are the 1 atm L(ol,pl,aug,hy) and L(pl,aug,hy,qz) (see Fig. 3c). For symbols see Fig. 4. See text for further discussion.

augite field may have extended to higher Qz, most likely due to H_2O in the liquid. Some volcanoes have hypersthene–phyric rocks that project in the olivine–plagioclase–augite field and others, with olivine phenocrysts, in the plagioclase–augite–hypersthene field, so magmas may have encountered L(ol,pl,aug,hy) when evolving at a range of pressures (or with a range of water contents) even at a single volcano.

Some magmas, particularly from the SNSP, that project into the 1-atm olivine–plagioclase–augite field have phenocrysts of plagioclase, augite, and hypersthene and probably crystallized at higher pressure. If liquids were anhydrous, a $P \sim 1$ kbar plausibly causes sufficient contraction of the olivine primary phase field for hypersthene–phyric rocks to plot in L(pl,aug,hy). Pressures of 2–3 kbar are required in the more likely case that liquids had low or moderate water contents (estimated from Baker & Eggler 1987).

Parental magmas of different volcanic suites probably had different K_2O contents at similar Ol but the range in K_2O was less than that produced after protracted crystallization (Fig. 5). Individual volcanoes define subparallel trends that are consistent with fractional crystallization of olivine + plagioclase + augite and then plagioclase + two pyroxenes. A liquid that remains in contact with olivine after reaching hypersthene-saturation is enriched in K_2O but its silica content increases slowly because of the shape of L(ol,pl,aug,hy). The lack of deflection of trends across Fig. 5 means that liquids did not remain on L(ol,pl,aug,hy) over large temperature ranges, presumably reflecting rapid separation of olivine

from hypersthene-saturated liquids. Thus, K_2O contents of evolved rocks are directly related to K_2O in their parental liquids.

The Or contents of SNSP rocks decrease slightly as Qz increases whereas separation of K-free phases should increase Or. This is not a decrease in K_2O but a more rapid increase in Qz than expected for separation of phenocryst phases, that is, K_2O does not increase as fast as it 'should'. Possibly, SNSP magmas evolved by fractional crystallization and assimilation of more silicic, less potassic igneous rocks.

ABSAROKITES, SHOSHONITES, AND BANAKITES

Lavas from the four Hiyoshi seamounts in the NNSP display very different LLD from those described in the previous section (Fig. 6). Samples from North Hiyoshi seamount (NH) are Ne-normative and each of the other seamounts has lavas very near the critical surface of silica-undersaturation. As a whole, the rocks form a trend largely in the anhydrous 1-atm plagioclase + augite field.

The NH rocks are mildly silica-undersaturated (Fig. 7). They contain phenocrysts of olivine, plagioclase, and augite and the most potassic rock contains biotite phenocrysts. Thus, a biotite field should be marked to indicate the path taken by biotite–phyric liquids; the location of that field is unknown.

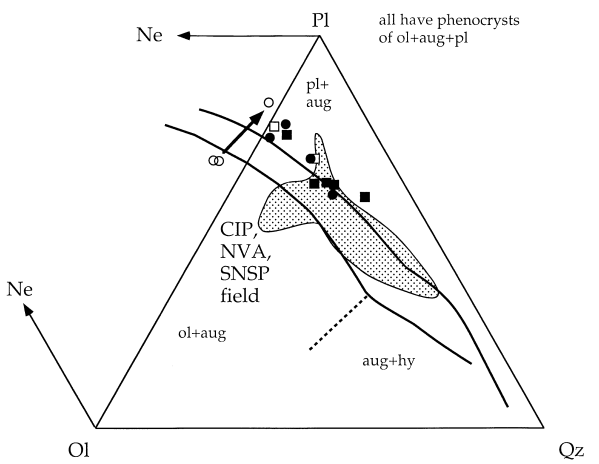

Fig. 6 Compositions of rocks from Hiyoshi seamounts (Bloomer *et al.* 1989), projected from Di onto Ne–Ol–Pl–Qz. In addition to ol + pl + aug, the most plagioclase-rich NH sample has biotite phenocrysts; the more silicic Ko-Hiyoshi sample has hornblende phenocrysts. The arrow between North Hiyoshi (NH) samples indicates the direction of evolution (as shown by major- and trace element contents of rocks). The field of Central Island Province (CIP), Northern Volcano Arc (NVA), and south Northern Seamount Province (SNSP) rocks from Fig. 4 is for comparison. (○), North Hiyoshi; (●), Central Hiyoshi; (■), South Hiyoshi; (□), Ko-Hiyoshi.

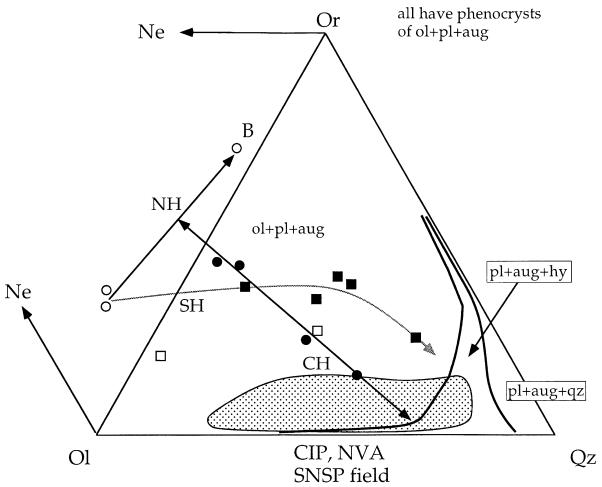

Fig. 7 Compositions of Hiyoshi rocks plotted on Fig. 6 projected from Pl and Di onto Ne–Ol–Or–Qz. North Hiyoshi (NH) samples define a trend with extreme increase in Or and slight decrease in silica-undersaturation (arrow marked NH). The 'B' denotes a biotite-bearing sample. The line CH denotes decrease in Or as that of Qz increases, a trend compatible with mixing alkaline and andesitic magmas. The shaded arrow labeled SH gives an interpretation of the evolution of these rocks by combined magma mixing and fractional crystallization beginning with a magma such as the alkaline parental liquid at NH. The field of Central Island Province (CIP), Northern Volcano Arc (NVA), and south Northern Seamount Province (SNSP) rocks from Fig. 5 is for comparison. For symbols see Fig. 6.

A limited variety of rocks was obtained from NH. Basalts have 1.2–1.5% K_2O; more evolved rocks have $\sim$4.5% K_2O; $Na_2O/K_2O < 1$. Bloomer *et al.* (1989) present a fractional crystallization model relating the two rock types. The fraction of liquid remaining from the parent in the derived liquid is $\sim$0.24, consistent with an almost four-fold increase in K_2O. Plagioclase and augite dominated a crystal assemblage that also included olivine and spinel. Lin *et al.* (1990) give the $^{87}Sr/^{86}Sr$ value of three NH samples and ε_{Nd} of two. The close agreement of isotopic compositions ($^{87}Sr/^{86}Sr = 0.70383$–$0.70387$; $\varepsilon_{Nd} = 2.6$, 2.9) is consistent with closed-system evolution of the magmas.

A trend due to crystallization of plagioclase, augite, and olivine and parallel to the critical surface resembles the experimental trend of Curtis (1991; Fig. 3d), and NH rocks occupy positions similar to those of type absarokites and type banakites of Iddings (1895) in projection (Meen & Curtis 1989). The NH magmas apparently evolved by fractional crystallization along the olivine–plagioclase–augite thermal divide.

The type banakites also possess biotite phenocrysts presumably because enrichment in H_2O and K_2O are coupled.

MIXED MAGMAS

CENTRAL HIYOSHI SEAMOUNT

The four Central Hyoshi seamount (CH) samples in projection define a near linear trend in which Or decreases as Qz increases (arrow labeled CH on Fig. 7). This trend is similar to that shown in Fig. 3(d) and is incompatible with separation of K-free phenocryst assemblages. It could be due to fractional crystallization of a potassic, silica-undersaturated assemblage but rocks have phenocrysts of olivine, plagioclase, augite, ± titanomagnetite. Precipitation of olivine, plagioclase, and augite from a CH magma with low Qz produces an LLD directly away from the Ol apex; in this case almost straight at Or. The actual trend of CH magmas is almost normal to a trend due to fractional crystallization of phenocryst phases. Bloomer *et al.* (1989) showed that compositions of the CH rocks are mathematically consistent with closed-system processes. The chemographic relations in Fig. 7 show such a model to be untenable. This is the case shown in Fig. 2. If the parent liquid is near the critical surface, the vector XA–PL–DL of Fig. 2 is subparallel to that surface (the join Ol–Or in projection) and the Qz-rich magmas at CH are well outside the closed-system tetrahedron.

A simple model consistent with chemographic relations is mixing between two magmas: one with low SiO_2, moderate K_2O; the other with higher SiO_2, low K_2O. Judging by the CH trend, the alkaline liquid involved in mixing could have been on the NH LLD between absarokites and banakites. The other end-member was silicic and may have been on L(ol,pl,aug,hy). The LLD at CIP, NVA, and SNSP (Fig. 5) cross L(ol,pl, aug,hy) near the CH trend so suitable magmas occurred both north and south of the Hiyoshi seamounts.

The less silicic CH magmas are phenocryst rich (10–25% augite, 20–25% plagioclase), suggesting some accumulation. These rocks fall in the plagioclase + augite field (Fig. 6) but are not far removed from the position of L(ol,pl,aug) unless they evolved at relatively high pressures, suggesting that only a small amount of the phenocryst population is accumulative. Note also that accumulation of plagioclase and augite does not move magma compositions along the CH trend but normal to it. Such marked crystallization of a mixed magma is consistent with mixing across a thermal divide. The curvature of the liquidus lines over a thermal divide can result in the resultant mixed magmas having temperatures well below those of their liquidi (Walker 1980).

In view of the small number of CH samples, we used a simple model of mixing. Straight lines were fitted to element–element data of NH and, separately, to those of CH. The intersection of the lines is taken as the composition of the alkaline end-member of mixing. The subalkaline end-member also lies on regression lines through the CH data but its positions on the lines are poorly constrained. The K_2O is zero on the K_2O-SiO_2 regression line for CH at 56.7% SiO_2, an upper bound on the SiO_2 content of the subalkaline magma. The K_2O is 0.4% at 55.5% SiO_2 and 1% at 53.8% SiO_2, reasonable limits on the SiO_2 content of that magma. Table 1 gives our chosen composition for the subalkaline magma and the amounts of end-members in each CH lava. We use these estimates to test whether trace element and isotopic data are consistent with a mixing model.

Contents of K_2O, Ba and LREE are all higher in rocks that contain more of the alkaline end-member (Fig. 8) and that have lower SiO_2. Variations in ratios of incompatible elements are even more indicative of magma mixing. The La/Yb ratio increases and the Ba/La ratio decreases as the amount of alkaline magma increases. Because these elements are quite incompatible in the phenocryst assemblages of these rocks, ratios of these elements to each other in the liquids can only be modified by huge amounts of crystallization or by open-system processes. The mixed rocks also have a range in ε_{Nd} with the alkaline end-member having lower ε_2 than the subalkaline end-member (Fig. 8).

Variations of compatible trace elements in CH rocks are not consistent with simple mixing in the way that incompatible trace elements are. The Cr (Fig. 8) and Ni contents are lower than expected from their contents in the end-members, assuming simple mixing. This plausibly reflects fractional crystallization (or accumulation) that accompanied mixing.

Table 1 Mixing at Central Hiyoshi seamounts

	Alkaline end-member	Subalkaline end-member	D52-1-1		D52-3-1		D51-3		D52-3-2	
			Real	Model	Real	Model	Real	Model	Real	Model
SiO_2	49.4	54.7	50.3	49.6	51.9	52.0	51.8	53.1	50.8	52.9
TiO_2	0.86	0.98	0.80	0.87	0.75	0.92	1.03	0.95	0.71	0.94
Al_2O_3	18.4	21.1	18.5	18.5	19.1	19.7	20.1	20.3	20.3	20.2
FeO*	9.02	8.02	8.54	8.99	8.15	8.54	8.60	8.33	7.55	8.35
MgO	5.13	2.61	4.23	5.07	3.29	3.92	3.18	3.38	3.15	3.45
CaO	9.73	8.55	9.31	9.07	8.94	9.16	8.70	8.91	9.00	8.94
Na_2O	2.95	3.50	2.97	2.97	3.62	3.21	3.32	3.33	3.38	3.32
K_2O	2.52	0.70	2.54	2.47	2.23	1.64	1.28	1.26	1.59	1.30
P_2O_5	0.29	0.23	0.34	0.29	0.28	0.26	0.26	0.25	0.28	0.25
Rb	57	5.5	65	56	53	32	23	21	32	23
Sr	1010	879	1015	1007	944	947	932	919	999	923
Ba	735	588	821	731	741	664	649	633	626	637
Zr	83.1	69.0	68	83	58	76	70	73	53	74
Y	21.8	24.2	21	22	18	23	24	24	23	23
Sc	28.8	9.9	21	28	19	20	13	16	17	16
V	309	195	271	306	211	254	221	230	203	233
Cr	38.6	16.5	9	38	20	28	17	23	10	24
Ni	25.4	0	11	25	8	13	5	8	15	8.6
La	40.5	27.7	42.5	40.2	38.3	34.3	32.2	31.6	n.d.	32.0
Ce	80.4	55.0	77.6	79.8	70.0	68.2	63.0	62.8	n.d.	63.6
Nd	34.8	28.0	34.7	34.6	30.6	31.5	30.4	30.1	n.d.	30.3
Dy	5.4	5.2	4.2	5.4	4.0	5.3	4.5	5.3	n.d.	5.3
Yb	1.9	2.3	2.0	2.0	2.1	2.1	2.2	2.2	n.d.	2.2
ε_{Nd}	2.5	4.5	2.4	2.5	2.9	3.4	3.8	3.8	n.d.	3.7
Fraction alkaline end-member	1	0		0.975		0.519		0.308		0.339

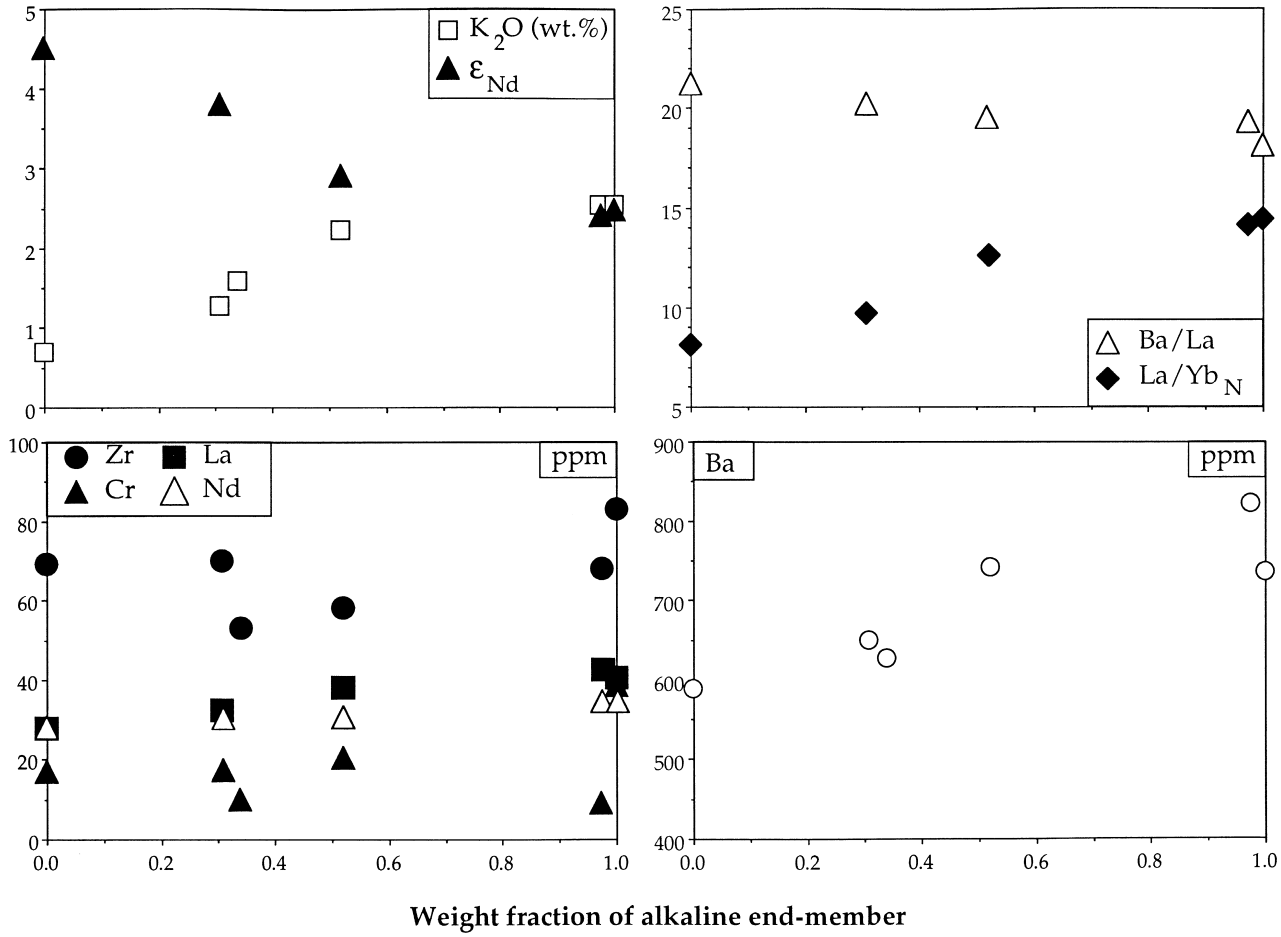

Fig. 8 Variations of contents of K_2O and trace elements, Ba/La and La_N/Yb_N, and ε_{Nd} with estimated weight fraction of alkaline end-member in central Hiyoshi rocks, calculated from a major-element model (Table 1). Values for estimated end-members are also shown.

SOUTH HIYOSHI AND KO-HIYOSHI SEAMOUNTS

The major-element contents of the South Hiyoshi seamount (SH) lavas are not consistent with simple magma mixing. Or contents of rocks with Ol:Qz > 1 are approximately equal but Or decreases as Qz increases thereafter (Fig. 7). The solid assemblage producing an LLD by fractional crystallization lies on the back-extension of that LLD so neither part of the trend is compatible with fractional crystallization of phenocrysts (olivine, plagioclase, augite). At least one mineral separating would have to be either potassic or silica-undersaturated mineral. The mafic part of the trend is only compatible with magma mixing if the silicic liquid was potassic and there is no evidence for the presence of such a magma.

The stippled line through the SH data represents coupled magma mixing and fractional crystallization. An alkaline magma (plausibly like a NH absarokite) mixed with low-K silicic magma and simultaneously crystallized olivine, plagioclase, and augite. The resultant LLD had a trend intermediate between those of the NH and CH lavas. Fractional crystallization waned and mixing waxed as magmas became more silicic (and viscosity increased) so the high-Qz part of the trend exhibits decreasing Or.

Element modeling of such a process is difficult because compositions of end-member magmas are unknown. Trace-element variations due to such a process differ from those due to fractional crystallization alone. Figure 9 shows variations of trace-element contents with the amount of Qz in the Ol–Or–Qz ternary. Ba, Rb, Zr, and K_2O reach maxima as Qz increases, and decrease after that. The limited rare earth element (REE) data show a similar increase in content at lower Qz. These data are consistent with a process dominated by fractional crystallization at lower

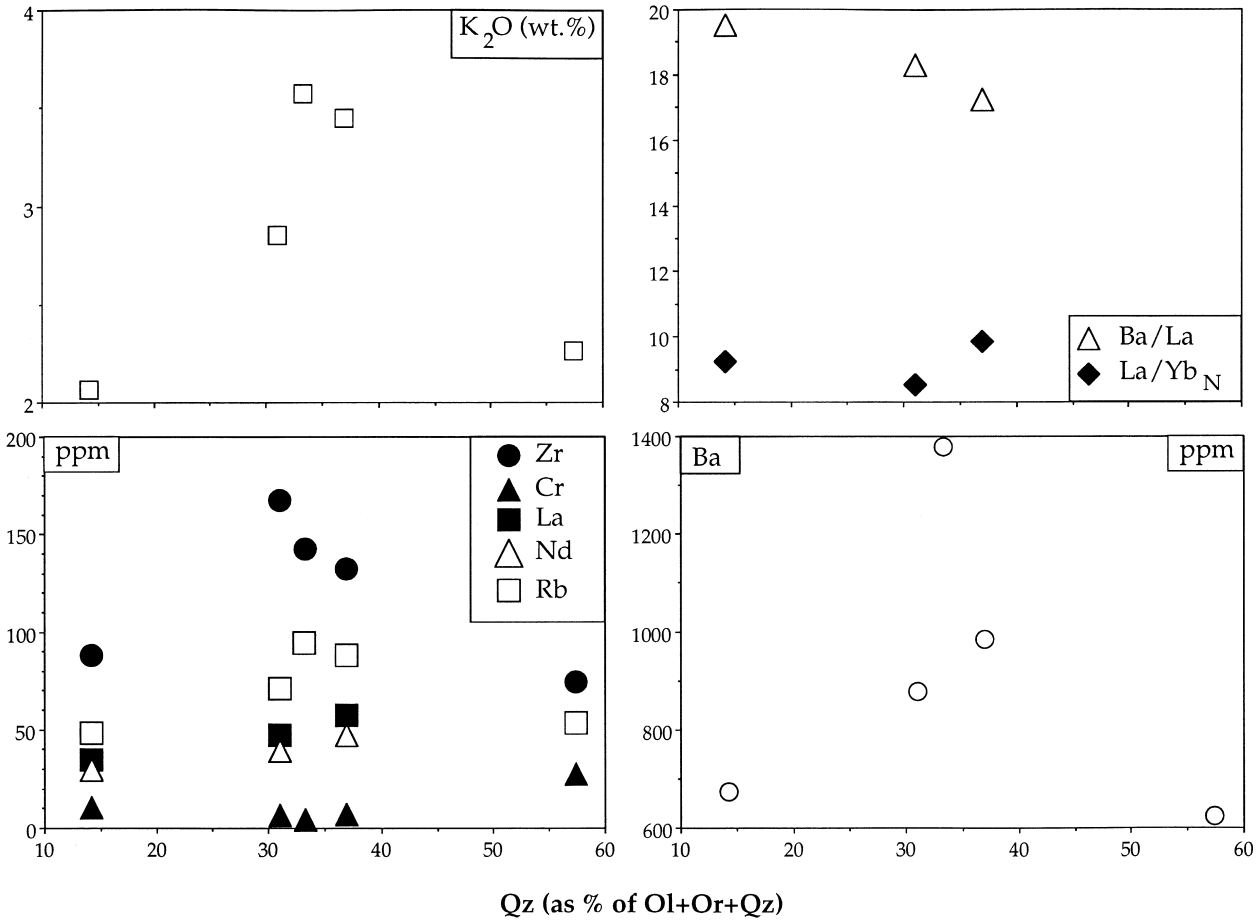

Fig. 9 Variations of contents of trace elements and Ba/La and La_N/Yb_N with Qz in South Hiyoshi rocks. Some incompatible trace elements reach maximum contents at an intermediate value of Qz. On the other hand, the content of Cr reaches a minimum at an intermediate value.

SiO_2 contents but involving addition of silicic material with lower LILE contents at higher SiO_2. The variation in the Ba/La ratio suggests that fractional crystallization alone cannot explain the trend. Lin *et al.* (1990) give two values of ε_{Nd} for SH lavas (3.5, 3.6) that are similar to values of CH lavas.

Only two data are available for Ko-Hiyoshi. The less silicic datum is near the critical surface of silica-undersaturation but is Hy-normative. Its MgO content and position on Fig. 6 preclude a major cumulate content and it may be a mixture of absarokite and subalkaline basalt. Evolution to andesite was not by simple fractional crystallization because the crystallizing assemblage would have been potassic, silica-undersaturated, or both. Evolution was plausibly by magma mixing coupled with fractional crystallization but the composition of the silicic end-member of mixing is very poorly constrained.

THE KASUGA SEAMOUNTS

Jackson (1989) presented data on two submarine volcanoes 20–50 km behind the arc front near Fukujin (Fig. 1). These are Kasuga 2 (K2) and Kasuga 3 (K3) seamounts. The chemistry of a single sample from Kasuga 1 (K1) seamount is included in the SNSP data discussed in the previous section.

Kasuga 2 seamount

Jackson (1989) gave compositions of whole rocks and glassy selvages from samples of the Kasuga seamounts. Eleven K2 lavas have phenocrysts of olivine, augite, and plagioclase; the other five have only olivine and augite. The Hy-normative K2 rocks lie on a single LLD compatible with control by olivine, plagioclase, and augite although displaced from the 1-atm L(ol,pl,aug) (Fig. 10). These rocks can therefore be interpre-

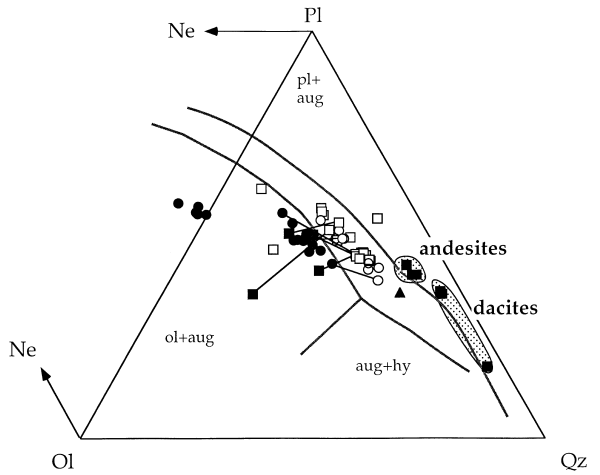

Fig. 10 Compositions of rocks from Kasuga seamounts projected from Di onto Ne–Ol–Pl–Qz. Data for K2 and K3 from Jackson (1989); K1 composition from Bloomer *et al.* (1989). Jackson (1989) gave analyses of both whole rocks and glasses. Lines join compositions of whole rocks and glasses in them. (▲), K1 whole-rock; (●), K2 whole-rock; (○) K2 glass; (■), K3 whole-rock; (□) K3 rock.

ted as the result of fractional crystallization in magma chambers at < 10 km.

The K2 rock trend projected from Pl and Di onto Ne–Ol–Or–Qz (Fig. 11) is not consistent with closed-system evolution. The K2 alkaline rocks are in a small field almost orthogonal to the critical surface. Or and Qz in Hy-normative rocks have a broad negative correlation with lower Or than CH

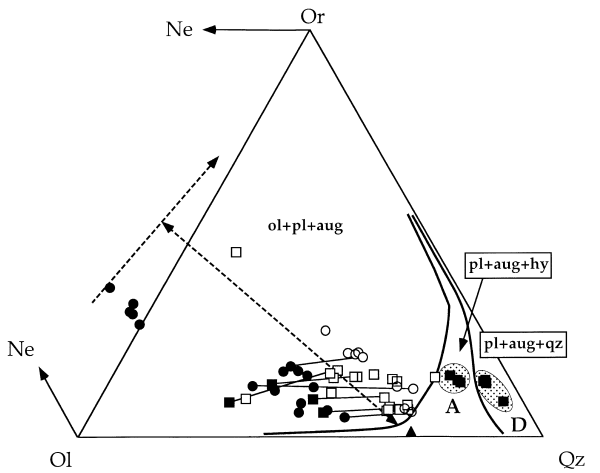

Fig. 11 Samples of Fig. 10 projected from Pl and Di onto Ne–Ol–Or–Qz. Lines join whole-rocks and glasses. K2 and K3 whole-rock data define a broad trend of decreasing Or as Qz increases. The glasses form a parallel trend. The one K1 sample has very low Or, projects into L(pl,aug,hy), and the rock contains phenocrysts of plagioclase and augite only. The dashed lines are the North Hiyoshi fractional crystallization trend and Central Hiyoshi mixing curve from Fig. 7, for comparison. For symbols see Fig. 10.

rocks. This broad trend is consistent with mixing between alkaline magmas and a low-K_2O, relatively silicic subalkaline magma. As some K2 basalts have $K_2O < 0.5\%$ so did the subalkaline end-member. Variation of SiO_2 in mixed rocks is very slight, so the subalkaline end-member had < 55% SiO_2. In addition, the small range in MgO (8.0–9.0%) in mixed rocks shows that the subalkaline magma was primitive. The most Ne-normative K2 magma, that projects very near the NH absarokite, plausibly represents the alkaline end-member for the low-Or portion of the trend. More potassic rocks may have formed from mixtures of more potassic alkaline liquids and a subalkaline magma. Alternatively, they formed by fractional crystallization of phenocryst minerals from mixed magmas.

Jackson (1989) also analysed glassy selvages of K2 rocks, and compositions of bulk rock and glass are available in some cases. Lines between glass and rock presumably indicate LLD due to *in situ* crystallization. Glass compositions projected from Di (Fig. 10) define a trend parallel to that of the whole rocks but shifted away from Ol so that it lies along the 1-atm L(ol,pl,aug). The glass–rock tie-lines on Fig. 11 are also consistent with crystallization of olivine, plagioclase, and augite but they are not parallel to the overall trend of the bulk rocks, consistent with formation of the rocks by magma mixing or by magma mixing and fractional crystallization.

The K2 rocks formed from magmas that were mixtures of Ne-normative basalts and low-K Hy-normative basalts. Mixed liquids were saturated in olivine and augite (but not plagioclase) and those minerals crystallized in shallow chambers to move residual liquids to the low-P L(ol,pl,aug). Separation of phenocrysts broadened the Qz–Or trend for subalkaline rocks by driving magmas along LLD of shallow slope on Fig. 11. The compositions of glassy selvages in the rocks extend the LLD to higher Qz contents.

Kasuga 3 seamount

Jackson (1989) analysed basalts from K3 and the glasses in them. Three of the four basalt analyses project to similar positions to subalkaline K2 basalts and presumably were similarly formed by mixing absarokite and basalt magmas. The other basalt has a much higher olivine content (Fig. 11), high MgO (14.6%) and modal olivine (10.6%) contents, suggesting that the lava accumulated olivine.

Most glass data for K3 are similar to those for K2 (Figs 10,11). We therefore believe that basalt evolution at K3 was similar to that at K2 although no alkaline magma is known from K3. One potassic glass (3.25% K_2O) is Hy-normative. Jackson (1989) does not give the composition of this bulk rock but indicates that it has more K_2O than the Ne-normative K2 basalts. If it formed from a mixed magma, the alkaline end-member was more potassic than the absarokites.

Igneous rocks at K3 include andesite (phenocrysts of plagioclase, two pyroxenes, magnetite, trace hornblende) and dacite (plagioclase–, hornblende–, magnetite–phyric). Andesites have similar major-element contents and project in a tight cluster (Figs 10,11). Projected compositions are consistent with formation by fractional crystallization of olivine, augite, and plagioclase and then plagioclase and pyroxenes from mixed magmas. Dacites are saturated in hornblende not augite, and do not lie in the same surfaces of Figs 10 and 11 as other samples; they are plotted for illustrative purposes. Dacites continue the trend of andesites without increase in Or. This may reflect separation of hornblende from more mafic liquids.

Stern *et al.* (1993) analysed Kasuga samples for Nd isotopic ratios (Fig. 12). The sole Ne-normative rock analysed has the lowest ε_{Nd} measured (and among the highest $^{87}Sr/^{86}Sr$). The four Hy-normative samples with the highest Or have $\varepsilon_{Nd} = 2.9$–3.4. Rocks with lower Or have higher ε_{Nd}. The most Or-poor rocks have $\varepsilon_{Nd} = 5.1$ and 6.1; the highest ε_{Nd} of any K2 or K3 samples. They plausibly represent the subalkaline mixing end-member. Andesites and dacites all have $\varepsilon_{Nd} = 4.7$. These felsic rocks formed from parental magmas that were mixtures of alkaline and subalkaline magmas, presumably by fractional crystallization, or they formed by remelting igneous rocks formed from such magmas. These data are consistent with formation of all Kasuga magmas by mixing an alkaline liquid ($\varepsilon_{Nd} \sim 3$) and a subalkaline liquid ($\varepsilon_{Nd} > 6$).

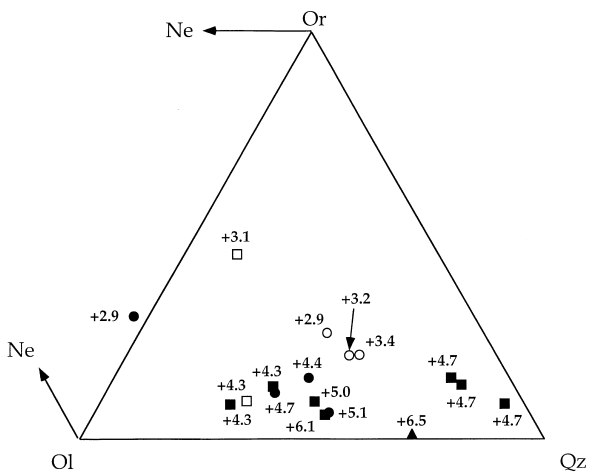

Fig. 12 Some samples shown on Fig. 11 with their values of ε_{Nd}. The one Ne-normative rock analysed isotopically has $\varepsilon_{Nd} = 2.9$, a value near that of the North Hiyoshi (NH) lavas and other Ne-normative rocks in the arc. The K1 lava has the highest ε_{Nd} of any Kasuga rock.

PRIMARY MAGMAS IN THE ARC

Results from the Hiyoshi and Kasuga regions indicate that subalkaline and alkaline magmas coexisted under at least two parts of the arc. The production of primary alkaline and subalkaline magmas beneath one area of the arc may throw light on the operation of subarc processes. Primary magmas of the subalkaline suites had limited ranges in major-element contents. Based on the high normative Ol in some multiply saturated subalkaline rocks (Fig. 4), primary magmas were mafic olivine tholeiite or calc-alkaline basalts that precipitated olivine (or olivine + plagioclase) to produce olivine–plagioclase–augite–phyric basalts parental to the subalkaline suites (Fig. 13). The olivine control line for Hy-normative compositions shown on Fig. 13 defines the highest Qz contents for primary magmas of at least some volcanoes. Those magmas precipitated olivine (and augite or plagioclase or both) to evolve to the most mafic Mariana basalts that are triply saturated, have Mg# = 58–63 and 30–50 p.p.m. Ni. Primary magmas formed at $P > 10$ kbar.

The most primitive magmas at North Hiyoshi are also multiply saturated and not primary (Fig. 13). An olivine control line from a postulated primary magma is subparallel to and near the control line for subalkaline magmas. Both lines cross peridotite melting curves at $P \geq 15$ kbar (Fig. 13). On that basis, alkaline and subalkaline primary magmas could represent melting of a source region at one pressure (≥ 15 kbar). The first liquids to form are silica-undersaturated; as the temperature is raised, liquids move toward the Ol–Qz join and become subalkaline. If the source contains amphibole or mica, the first-formed melt is more alkaline.

Magmagenesis models must account for trace element and isotopic compositions of the rocks.

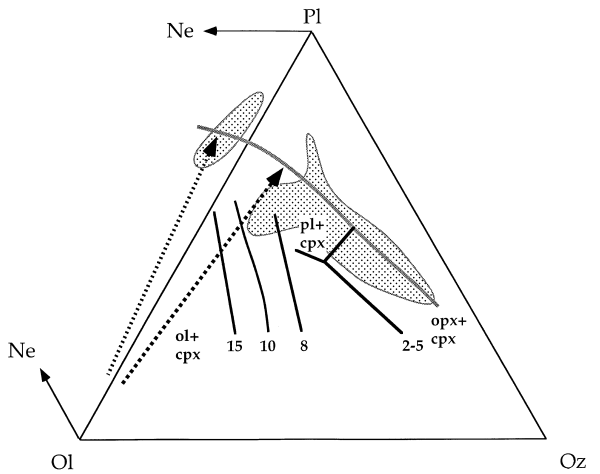

Fig. 13 Comparison of postulated liquid line of descent (LLD) of Mariana magmas with experimentally determined melts of anhydrous peridotite. Gray line is approximate position of L(ol,pl,aug). Fields are for multiply saturated Central Island Province (CIP), Northern Volcano Arc (NVA), and south Northern Seamount Province (SNSP) rocks (Hy-normative) and for North Hiyoshi (NH) lavas (Ne-normative). A dashed line from each field is an olivine control line that could represent paths of liquids after separation from the mantle and is not in the plane of projection. Solid lines show liquids in equilibrium with olivine, Ca-rich clinopyroxene, and orthopyroxene at different pressures (kbar at the ends of the lines). At < 5 kbar, liquids form in equilibrium with plagioclase lherzolite so a pseudo-eutectic is shown; other lines are for liquids in equilibrium with lherzolite only.

The alkaline magmas formed from a source with higher contents of more incompatible elements and lower ε_{Nd}. They cannot be explained by different degrees of melting of the same homogeneous source. In addition, the model must be consistent with the coeval presence of two magmas derived from different primary liquids at the Hiyoshi and Kasuga seamounts.

A hydrous or otherwise enriched mantle melts at lower temperature than less fertile mantle and, at a given temperature, produces more liquid. The two liquids have similar silica-saturations at a given pressure and temperature for the same residual mineral assemblage, no matter what the source composition. The difference between the two primary liquids on Fig. 13, if due to isobaric melting, requires a temperature contrast over a short distance (~7 km separate North Hiyoshi and Central Hiyoshi). Alternatively, alkaline magmas formed from hydrous enriched mantle that rose beneath certain parts of the arc. Other parts of the subarc mantle melted under the influence of slab-derived fugitive phases at shallower levels and, probably, with higher liquid fractions. Uncertainties in knowledge of source compositions and other parameters does not allow quantification of figures for depth and temperature of melting.

CONCLUSIONS

Many volcanic suites in the Mariana and Volcano arcs follow LLD consistent with low-pressure fractional crystallization of phenocrysts (olivine, plagioclase, augite, ± hypersthene, ± titanomagnetite) to cause silica-enrichment as magmas evolved from basalt to andesite to dacite. These data could also result from magma mixing but mixing was between mafic and felsic magmas on similar LLD.

Primary magmas at North Hiyoshi also crystallized olivine, plagioclase, and augite, but the LLD differed greatly from those just mentioned. It parallels the critical surface of silica-undersaturation and was plausibly along the olivine–plagioclase–augite thermal divide. This causes silica-enrichment but leaves silica saturation unchanged while causing enrichment in incompatible elements.

Compositional arrays of rock compositions at each of the other Hiyoshi seamounts and neighboring edifices cannot be explained by fractional crystallization alone. Alkaline and subalkaline liquids coexisted at each center and the influence of alkaline magmas apparently waned at edifices successively further from North Hiyoshi. At Central Hiyoshi, ~7 km south of North Hiyoshi, magmas formed by mixing alkaline and subalkaline magmas with minor fractional crystallization. At South Hiyoshi and Ko-Hiyoshi, further south, magmas formed by combined magma mixing and fractional crystallization.

The Kasuga 2 and 3 seamounts are 20–50 km behind the arc front. Ne-normative rocks are present only at K2 but all Hy-normative magmas at the seamounts apparently formed by mixing.

The Hiyoshi seamounts are north of the point at which the extension axis of the back-arc basin Mariana Trough intersects the arc (Fig. 1). Stern *et al.* (1984) and Bloomer *et al.* (1989) postulated that the back-arc rift propagates northward into the arc near the junction of the Mariana and Volcano arcs, causing extension in the arc and subarc mantle and resulting in tapping new mantle sources. They proposed there would be a progression from pre-rift tholeiitic or calc-alkaline magmatism to a phase of alkalic magmatism

with gradual return to subalkaline volcanism as the site of rifting moves away from that particular volcano.

Although the petrogenetic models described for the suites at several of the Hiyoshi seamounts are based on a few points, these suites did not form by closed-system separation of their phenocrysts. Attempts to interpret these rocks within a framework inferred from compositions of rocks in the arc must necessarily yield erroneous models for their origin.

ACKNOWLEDGEMENTS

This paper benefitted from reviews by J. Hawkins, D. Elthon that resulted in a greatly improved manuscript.

REFERENCES

Baker D. R. & Eggler D. H. 1987. Compositions of anhydrous and hydrous melts coexisting with plagioclase, augite, and olivine or low-Ca pyroxene: Application to the Aleutian volcanic center of Atka. *American Mineralogist* **72**, 12–28.

Bloomer S. H., Stern R. J., Fisk E. & Geschwind C. H. 1989. Shoshonitic volcanism in the northern Mariana 1. Mineralogic and major and trace element characteristics. *Journal of Geophysical Research* **78**, 4469–96.

Chow T. J., Stern R. J. & Dixon T. H. 1980. Absolute and relative abundances of K, Rb, Sr, and Ba in circum-Pacific island-arc magmas, with special reference to the Marianas. *Chemical Geology* **28**, 111–21.

Curtis P. C. 1991. Competing magmatic processes at a continental rift: Petrology and geochemistry of Quaternary volcanoes in the Turkana rift zone, East Africa. PhD Thesis, University of North Carolina, Chapel Hill, North Carolina, USA.

Dixon T. H. & Batiza R. 1979. Petrology and chemistry of recent lavas in the Northern Marianas: Implications for the origin of island arc basalts. *Contributions to Mineralogy and Petrology* **70**, 167–81.

Dixon T. H. & Stern R. J. 1983. Petrology, chemistry and isotopic composition of submarine volcanoes in the southern Mariana arc. *Geological Society of America Bulletin* **94**, 1159–72.

Edwards C., Menzies M. & Thirlwall M. 1991. Evidence from Muriah, Indonesia, for the interplay of supra-subduction zone and intraplate processes in the genesis of potassic alkaline magmas. *Journal of Petrology* **32**, 555–92.

Garcia M. O., Liu N. W. K. & Muenow D. W. 1979. Volatiles in submarine volcanic rocks from the Mariana Island arc and trough. *Geochimica et Cosmochimica Acta* **43**, 305–12.

Hole M. J., Saunders A. D., Marriner G. F. & Tarney J. 1984. Subduction of pelagic sediments: Implications for the origin of Ce-anomalous basalts from the Mariana islands. *Journal of the Geological Society of London* **141**, 453–72.

Hussong D. M. & Uyeda S. 1981. Tectonic processes and the history of the Mariana arc: A synthesis of the results of Deep Sea Drilling Project leg 60. *In Initial Reports of the Deep Sea Drilling Project*, **60**, pp. 909–29. College Station, TX, USA.

Iddings J. P. 1895. Absarokite–shoshonite–banakite series. *Journal of Geology* **3**, 935–59.

Ito E. & Stern R. J. 1986. Oxygen- and strontium-isotopic investigations of subduction zone volcanism: The case of the Volcano arc and the Marianas Island Arc. *Earth and Planetary Science Letters* **76**, 312–20.

Jackson M. C. 1989. Petrology and petrogenesis of recent submarine volcanics from the northern Mariana arc and back-arc basin. PhD Thesis, University of Hawaii, Hawaii, USA.

Jackson M. C. 1993. Crystal accumulation and magma mixing in the petrogenesis of tholeiitic andesites from Fukujin Seamount, northern Mariana island arc. *Journal of Petrology* **34**, 259–89.

Lin P-N., Stern R. J. & Bloomer S. H. 1989. Shoshonitic volcanism in the northern Mariana Arc 2. Large-ion lithophile and rare earth element abundances: Evidence for the source of incompatible element enrichments in intraoceanic arcs. *Journal of Geophysical Research* **78**, 4497–514.

Lin P-N., Stern R. J., Morris J. & Bloomer S. H. 1990. Nd- and Sr-isotopic compositions of lavas from the northern Mariana and southern Volcano arcs: Implications for the origin of island arc melts. *Contributions to Mineralogy and Petrology* **105**, 381–92.

Martinez F., Fryer P., Baker N. A. & Yamazaki T. 1995. Evolution of backarc rifting: Mariana Trough 20–24N. *Journal of Geophysical Research* **100**, 3807–27.

Meen J. K. 1990. Elevation of potassium content of basaltic magma by fractional crystallization: The effect of pressure. *Contributions to Mineralogy and Petrology* **104**, 309–31.

Meen J. K. & Curtis P. C. 1989. What are shoshonites? *Eos Transactions of the American Geophysical Union* **70**, 1421.

Meijer A. 1976. Pb and Sr isotopic data bearing on the origin of volcanic rocks from the Mariana island-arc system. *Geological Society of America Bulletin* **87**, 1358–69.

Meijer A. 1980. Primitive arc volcanism and a boninite series: Examples from western Pacific island

arcs. *In* Hayes D. E. ed. The Tectonic and Geologic *Evolution of Southeastern Asia's Seas and Islands*, Part 2, pp. 255–69. American Geophysical Union, Washington DC.

Meijer A. & Reagan M. 1981. Petrology and geochemistry of the island of Sarigan in the Mariana Arc: Calc-alkaline volcanism in an oceanic setting. *Contributions to Mineralogy and Petrology* **77**, 337–54.

Morse S. A. 1980. *Basalts and Phase Diagrams*. Springer-Verlag, Heidelberg.

Plank T. & Langmuir C. H. 1988. An evaluation of the global variations in the major element chemistry of arc basalts. *Earth and Planetary Science Letters* **90**, 349–70.

Reagan M. & Meijer A. 1984. Geology and geochemistry of early arc-volcanic rocks from Guam. *Geological Society of America Bulletin* **95**, 701–13.

Sack R. O., Carmichael I. S. E., Rivers M. & Ghiorso M. S. 1980. Ferric–ferrous equilibria in natural silicate liquids at 1 bar. *Contributions to Mineralogy and Petrology* **75**, 369–76.

Shand S. J. 1927. *The Eruptive Rocks*. Wiley, New York.

Stern R. J. 1979. On the origin of andesite in the Northern Mariana arc: Implications from Agrigan. *Contributions to Mineralogy and Petrology* **68**, 207–19.

Stern R. J. 1981. A common mantle source for western Pacific island arc and 'hot-spot' magmas: Implications for layering in the upper mantle. *YearBook Carnegie Institution of Washington* **80**, 455–61.

Stern R. J. 1982. Strontium isotopes from circum-Pacific island arcs and marginal basins: Regional variations and implications for magmagenesis. *Geological Society of America Bulletin* **93**, 477–86.

Stern R. J. & Bibee L. 1984. Esmeralda Bank: Geochemistry of an active submarine volcano in the Mariana Island arc. *Contributions to Mineralogy and Petrology* **86**, 159–69.

Stern R. J. & Ito E. 1983. Trace-element and isotopic constraints on the source of magmas in the active Volcano and Mariana island arcs, western Pacific. *Journal of Volcanology and Geothermal Research* **18**, 461–82.

Stern R. J., Smoot N. C. & Rubin M. 1984. Unzipping of the Volcano arc, Japan. *Tectonophysics* **102**, 153–74.

Stern R. J., Jackson M. C., Fryer P. & Ito E. 1993. O, Sr, Nd and Pb isotopic composition of the Kasuga Cross-Chain in the Mariana Arc: A new perspective on the K–h relationship. *Earth and Planetary Science Letters* **119**, 459–75.

Walker D. 1980. Phase equilibrium curvature effects on mixed magma. *Eos Transactions of the American Geophysical Union* **61**, 67.

White A. J. R. & Chappell B. W. 1977. Ultrametamorphism and granitoid genesis. *Tectonophysics* **43**, 7–22.

White W. M. & Patchett J. 1984. Hf–Nd–Sr isotopes and incompatible element abundances in island arcs: Implications for magma origins and crust–mantle evolution. *Earth and Planetary Science Letters* **29**, 167–85.

Wood D. A., Marsh N. G., Tarney J., Joron J. L., Fryer P. & Treuil M. 1981. Geochemistry of igneous rocks recovered from a transect across the Mariana Trough, Fore-arc, and Trench, sites 453 through 461, Deep Sea Drilling Project leg 60. *In* Hussong D. M. *et al.* eds. *Initial Reports of the Deep Sea Drilling Project*, **60**, pp. 611–33. College Station, TX, USA.

Woodhead J. D. 1989. Geochemistry of the Mariana arc (western Pacific): Source composition and processes. *Chemical Geology* **76**, 1–24.

Woodhead J. D. & Fraser D. G. 1985. Pb, Sr, and Be isotopic studies of volcanic rocks from the northern Mariana islands: Implications for magma genesis and crustal recycling in the western Pacific. *Geochimica et Cosmochimica Acta* **49**, 1925–30.